



Ionic liquid-based zwitterionic organic polymer monolithic column for capillary hydrophilic interaction chromatography

Journal:	<i>Analyst</i>
Manuscript ID:	AN-ART-04-2015-000662.R1
Article Type:	Paper
Date Submitted by the Author:	16-May-2015
Complete List of Authors:	Wang, Tingting; Ningbo University of Technology, College of Chemical Engineering Chen, Yihui; Xiangshan Entry-Exit Inspection and Quarantine, Ma, Junfeng; The Johns Hopkins University School of Medicine, Zhang, Xiaodan; Dalian Institute of Chemical Physics, Chinese Academy of Sciences, Zhang, Lihua; Dalian Inst Chem Phys, Zhang, Yukui; Dalian Institute of Chemical Physics, Chinese Academy of Sciences,

1
2
3
4 **Ionic liquid-based zwitterionic organic polymer monolithic**
5
6 **column for capillary hydrophilic interaction chromatography**
7
8

9
10 Tingting Wang, ^{*a} Yihui Chen, ^c Junfeng Ma, ^d Xiaodan Zhang, ^b Lihua Zhang ^b and Yukui Zhang ^b
11

12
13
14 ^a *College of Chemical Engineering, Ningbo University of Technology, Ningbo 315016, China.*

15 *E-mail: wangtingting@nbut.edu.cn; Fax: +86 574 65756710; Tel.: +86 574 65756733.*
16

17
18 ^b *Key Laboratory of Separation Science for Analytical Chemistry, National Chromatographic*
19 *Research and Analysis Center, Dalian Institute of Chemical Physics, Chinese Academy of Sciences,*
20 *Dalian 116023, China.*

21
22 ^c *Xiangshan Entry-Exit Inspection and Quarantine, Xiangshan 310014, China.*
23

24
25 ^d *Department of Biological Chemistry, The Johns Hopkins University School of Medicine,*
26 *Baltimore, MD 21205, USA.*
27
28
29
30
31
32
33
34
35
36
37
38
39
40
41
42
43
44
45
46
47
48
49
50
51
52
53
54
55
56
57
58
59
60

1
2
3
4
5
6
7
8
9
10
11
12
13
14
15
16
17
18
19
20
21
22
23
24
25
26
27
28
29
30
31
32
33
34
35
36
37
38
39
40
41
42
43
44
45
46
47
48
49
50
51
52
53
54
55
56
57
58
59
60

In current study, a novel ionic liquid-based zwitterionic organic polymer monolithic column was developed, by copolymerizing 1-vinyl-3-(butyl-4-sulfonate) imidazolium, acrylamide and *N, N'*-methylenebisacrylamide in a quaternary porogenic solvent consisting of formamide/dimethyl sulphoxide/polyethylene glycol 8,000/polyethylene glycol 10,000, for capillary hydrophilic interaction chromatography. The monolithic stationary phase was optimized by adjusting the amount of monomers in the polymerization solution along with the composition of porogenic solvent. The optimized monolith exhibited excellent selectivity and favorable retention for nucleosides and benzoic acid derivatives. Primary factors affecting the separation efficiency of the monolithic column (including acetonitrile content, pH, and buffer salt concentration in mobile phase) have been thoroughly evaluated. Excellent reproducibility of retention time for five nucleosides was achieved, with relative standard deviations of run-to-run (n=3), column-to-column (n=3) and batch-to-batch (n=3) in the range of 0.18-0.48%, 2.33-4.20% and 3.07-6.50%, respectively.

1. Introduction

As a complementary to reversed-phase liquid chromatography (RPLC), hydrophilic interaction chromatography (HILIC) has gained significant popularity for polar compounds separation in recent years. HILIC is characterized as normal-phase chromatography on polar columns in aqueous-organic mobile phases rich in organic solvents. Similar to RPLC, the mobile phase of HILIC dissolves hydrophilic analysts. However, the limited types of sorbents currently available have hampered the separation of polar and hydrophilic compounds with complexity and diversity. To date, several kinds of stationary phases have been developed to serve as the HILIC sorbents [1, 2], among which zwitterionic stationary phase is a very appealing one [3, 4].

Ionic liquid has gained increasing interest in the field of analytical chemistry due to their unique properties such as variable viscosity, negligible vapor pressure, high thermal stability, multiple salvation interaction, and designability of structure and physicochemical properties, etc. Besides being used as mobile-phase additives [5-7], ionic liquids demonstrate almost perfect properties as modifier of silica sorbents in LC separation. A series (~20 types) of surface-confined ionic liquids stationary phase, including the imidazolium zwitterionic stationary phase have been described [8, 9]. In addition, Qiu et al. developed a silica-based 1-alkyl-3-(propyl-3-sulfonate) imidazolium zwitterionic stationary phase, exhibiting multiple retention mechanisms, such as anion-exchange, electrostatic attraction and repulsion interactions, and hydrophobic interaction [10]. However, the applicability of the developed imidazolium zwitterionic stationary phase for HILIC separation was demonstrated only recently. With the IL-modified silica zwitterionic material prepared by the copolymerization of anionic and cationic monomers, Qiu et al. [11] separated polar compounds under the HILIC mode. Shortly afterwards, 1-vinyl-3-(butyl-4-sulfonate) imidazolium was grafted onto the surface of 3-mercaptopropyl modified silica particles by “thiol-ene” click chemistry [12], with the column efficiency measured with cytosine as solute. Of note, silica particles are the main matrix for the preparation of imidazolium zwitterionic stationary phases in these studies, in which excellent

1
2
3 separation efficiency under HILIC mode was observed.
4

5 Compared with the traditionally used silica-based packed column, monolithic
6 column is becoming a prevalent approach due to its advantages, such as the easy
7 control of permeability, no need to prepare frits, and higher phase ratios [13]. Several
8 methacrylate-based monolithic columns have been prepared for hydrophilic
9 interaction liquid chromatography separation [14, 15]. Moreover, although several
10 ionic liquid-based monolithic columns have been recently reported, these columns
11 were just used for capillary electrochromatography [16, 17]. The applicability of ionic
12 liquid-based organic polymer monoliths for HILIC separation has been rarely
13 explored [18].
14
15
16
17
18
19
20
21

22 In this study, an ionic liquid-based monolithic stationary phase was synthesized
23 by single-step copolymerization of 1-vinyl-3-(butyl-4-sulfonate) imidazolium
24 (VBSIm), acrylamide (AM) and *N, N'*-methylenebisacrylamide (MBA). The
25 composition of the poly (VBSIm-AM-MBA) monolith was thoroughly optimized.
26 The resulting zwitterionic monolithic column was applied for the separation of
27 nucleosides and benzoic acid derivatives under HILIC mode, with excellent
28 separation efficiency and reproducibility achieved.
29
30
31
32
33
34
35
36
37

38 **2. Materials and methods**

39 **2.1 Reagents and materials**

40 Acrylamide (AM) and *N, N'*-methylenebisacrylamide (MBA) were purchased from
41 J&K Scientific Ltd (Shanghai, China). 1-Vinyl-3-(butyl-4-sulfonate) imidazolium
42 (VBSIm, 99%) was obtained from Shanghai Chengjie Chemical Co., Ltd (Shanghai,
43 China). Azobisisobutyronitrile was purchased from Sinopharm Chemical Reagent Co.,
44 Ltd (Shanghai, China). Acetonitrile (ACN, LC grade) was obtained from Tedia
45 (Fairfield, OH, USA). 3-Methacryloxypropyltrimethoxysilane was purchased from
46 Sigma (St. Louis, MO, USA). Polyethylene glycol (PEG) with molecular weight
47 8,000 and 10,000, formamide, dimethyl sulphoxide (DMSO), ammonium formate and
48 formic acid were all purchased from Aladdin (Shanghai, China). Benzoic acid
49
50
51
52
53
54
55
56
57
58
59
60

1
2
3 derivatives including 4-hydroxybenzoic acid (4-HBA), 3-hydroxybenzoic acid
4 (3-HBA), and 3,4- dihydroxybenzoic acid (3, 4-DHBA) were purchased from Aladdin
5 (Shanghai, China). Melamine was obtained from Agro-Environmental Protection
6 Institute, Ministry of Agriculture (Tianjin, China). Nucleosides including adenosine,
7 uridine, cytosine, inosine and cytidine were all purchased from J&K Scientific Ltd
8 (Shanghai, China). The water used throughout all experiments was supplied by a
9 Milli-Q system (Millipore, Molsheim, France). The polyimide-coated fused-silica
10 capillaries (150 μm i.d. \times 375 μm o.d.) were obtained from Yongnian Optical Fiber
11 Factory (Hebei, China). For optimization of HILIC separation conditions, each
12 benzoic acid derivatives was at concentration of 3.3 $\mu\text{g}\cdot\text{mL}^{-1}$, and adenosine, uridine,
13 cytosine, inosine and cytidine was at concentration of 5.0, 10.0, 5.0, 10.0 and 10.0
14 $\mu\text{g}\cdot\text{mL}^{-1}$, respectively.
15
16
17
18
19
20
21
22
23
24
25
26
27

28 **2.2 Instrumentation**

29 The scanning electron micrographic images of the organic polymer monolithic
30 column were carried out on a Hitachi S-4800 scanning electron microscope (Tokyo,
31 Japan). Evaluation of the monolithic columns were performed on Calmflow-S100
32 capillary LC system containing UV detector with a 35 nL micro flow cell, one nano
33 valve with two position (Valco Instruments Co., Inc, USA), a vacuum degasser, a
34 binary pump and a data acquisition module (Lumtech, Germany). The permeability of
35 monolithic columns was measured using a high pressure HPLC pump under constant
36 pressure (Dalian Elite Analytical Instruments Co., Ltd, China).
37
38
39
40
41
42
43
44
45

46 **2.3. Preparation of the monolithic column**

47 In order to prepare polymer monolith in situ, a fused silica capillary was treated with
48 3-Methacryloxypropyltrimethoxysilane according to our previous report [19]. The
49 poly (VBSIm-AM-MBA) monolith was synthesized via one-step polymerization (Fig.
50 1). To avoid decomposition of VBSIm, 33.4 mg VBSIm was dissolved in 408.0 mg
51 formamide immediately by vortexed. Subsequently, 10.0 mg AM, 20.0 mg MBA,
52 204.0 mg DMSO, 22.5 mg PEG-8,000 and 40.5 mg PEG-10,000 were added into the
53
54
55
56
57
58
59
60

1
2
3
4
5
6
7
8
9
10
11
12
13
14
15
16
17
18
19
20
21
22
23
24
25
26
27
28
29
30
31
32
33
34
35
36
37
38
39
40
41
42
43
44
45
46
47
48
49
50
51
52
53
54
55
56
57
58
59
60

mixture, and then mixed completely homogeneous by ultrasonication. After adding 1.0 mg initiator azobisisobutyronitrile, the solution was vortexed to obtain homogeneous solution, and purged with N₂ for 2 min. The pretreated capillary was filled with the mixture, and then plugged at the both ends with silicon rubber for polymerization at 75 °C for 20 h. Finally, the prepared monolithic column was rinsed with methanol to flush out unreacted reagents.

2.4. Chromatographic conditions

The HILIC method for benzoic acid derivatives was isocratic with a mobile phase of (A) 6% 20 mmol/L ammonium formate (pH 3.0) and (B) 94% acetonitrile. The HILIC method for nucleosides was isocratic with a mobile phase of (A) 8% 20 mmol/L ammonium formate (pH 4.0) and (B) 92% acetonitrile. The chromatograms of all analytes were set at 214 nm, and the flow rate was 1.2 μL min⁻¹. The injection volume was 0.2 μL. The capillary monolithic column was 30 cm total length.

3. Results and discussion

3.1 Preparation and characterization of the monolithic column

In our previous work, 1-aminopropyl-3-methylimidazolium chloride was successfully grafted onto a poly (glycidyl methacrylate-AM-MBA) monolithic column, which showed a mixed mode of hydrophobicity and anion-exchange capability [20]. In this study, a zwitterionic compound, namely VBSIm, was used to increase the hydrophilicity of the monolithic column. Interestingly, a colorless liquid was obtained when VBSIm was dissolved in formamide immediately. However, with the increase of time (e.g., >3 min), the solution color turned to primrose yellow (the color of 1-vinylimidazole and 1,4-butane). Thus, VBSIm immediately dissolved in the formamide was used to avoid decomposition. Because of the relatively insolubility of MBA in formamide, DMSO was introduced as porogen to enhance the solubility of MBA. To investigate the effect of the composition of the DMSO on the preparation of poly (VBSIm-AM-MBA) monolith, the ratio of formamide/DMSO (w/w) was varied

1
2
3 from 1 (column 1) to 5 (column 3), with the other composition kept constant. As
4 shown in Table 1, only column 2 (with a ratio of formamide/DMSO of 2) yielded a
5 uniform monolithic structure with reasonable permeability, compared to the other two
6 columns whose permeability could not be determined due to the high backpressure of
7 column 1 and a slack continuous bed of column 3.
8
9

10
11
12 Since monomers and cross-linkers can often be dissolved well in ternary
13 porogenic solvents, quaternary porogenic solvent systems have rarely been adopted
14 for the preparation of the polymer monoliths [13, 21]. Herein, the effect of the ratio of
15 PEG-8,000/PEG-10,000 (w/w) was investigated (column 2, 4-7). The permeability
16 was increased with the decrease of the ratio of PEG-8,000/PEG-10,000, which is in
17 agreement with a previous report [22], with the maximum column efficiency obtained
18 with a ratio of 25/45. As a result, a ternary porogenic system including PEG-8,000 and
19 PEG-10,000 (with a ratio of 25/45) was used to achieve the best column efficiency.
20
21
22

23
24
25 The ratio of monomers, AM and VBSIm, also influences the permeability and
26 column efficiency. As shown in Table 1, the permeability of column was decreased
27 with the increase of VBSIm composition (column 6, 8-11). When the composition
28 (column 11) of VBSIm was 100%, the monolithic column became almost
29 impermeable that could withstand a pressure high up to 30 MPa. According to its
30 formula, VBSIm contains a butanesulfonic acid group and an imidazole group, which
31 could be assumed as a long carbon chain modified AM. Since chemical modification
32 affects monolith porosity without changing the monolith skeleton integrity [23], an
33 increased amount of VBSIm might lead to an enhanced chemical modification effect
34 and thus high backpressure of the monolithic column. As a result, a 10/33.4 (w/w) of
35 AM/VBSIm was selected in the following studies in order to achieve the best
36 permeability and column efficiency.
37
38
39
40
41
42
43
44
45
46
47
48
49

50
51 In order to further improve column efficiency, we tried to increase the ratio of
52 monomers to porogens. However, an increased ratio also resulted in decreased
53 permeability of certain columns (column 6, 12 and 13; Table 1). Since the
54 polymerization solution with a monomer/porogenic solvent ratio of 63.4/675 (w/w)
55 yielded a monolithic column (column 12) with the highest column efficiency and
56
57
58
59
60

1
2
3
4
5
6
7
8
9
10
11
12
13
14
15
16
17
18
19
20
21
22
23
24
25
26
27
28
29
30
31
32
33
34
35
36
37
38
39
40
41
42
43
44
45
46
47
48
49
50
51
52
53
54
55
56
57
58
59
60

excellent permeability. Thus, the composition of polymerization reagents of column 12 was adopted in further experiments. To further evaluate the effect of VBSIm on the HILIC separation efficiency, we prepared a poly (AM-MBA) monolithic column (column 14; Table 1), which showed much lower column efficiency than that of column 12. Apparently, VBSIm plays an important role in the HILIC separation of polar compounds.

The morphology of the optimized poly (VBSIm-AM-MBA) monolithic column was examined by scanning electron microscopy (Fig. 2). The monolithic material was well attached to the inner wall of capillary (Fig. 2A). And the through-pore size was ranged from 0.5 to 2 μm , which could provide high permeability and low backpressure (Fig. 2C). Moreover, the monolithic material contained homogeneous micro-globules and uniform nanopores (Fig. 2B), which could render high separation efficiency.

3.2 Chromatographic evaluation of poly (VBSIm-AM-MBA) monolithic column for HILIC

Nucleosides and benzoic acid derivatives, which are commonly used to evaluate the selectivity of HILIC stationary phases [24, 25], were chosen as model compounds to investigate the chromatographic property of the poly (VBSIm-AM-MBA) monolithic column. Log p and pK_a of elected nucleosides and benzoic acid derivatives are shown in Table 2. Since the separation efficiency of HILIC was affected by parameters including organic modifier content, buffer pH and buffer salt concentration in the mobile phase, we optimized these parameters thoroughly.

ACN/water mobile phase is most commonly used for HILIC separation. With a constant salt concentration of 20 mM ammonium formate (pH 3.0), the effect of ACN content on retention factor (k') was investigated. As shown in Fig. 3, retention factor of all nucleosides and benzoic acid derivatives was increased with the increase of the ACN content, indicating a typical HILIC retention mechanism. Nucleosides and benzoic acid derivatives were almost un-retained when the ACN content was less than 75% and 90%, respectively. However, all analytes emerged with broad peaks or were

1
2
3 not eluted when ACN content was higher than 92% for nucleosides and 95% for
4 benzoic acid derivatives. The interesting phenomenon may be explained by the
5 solubility limitations of these analytes [26]. With a mobile phase composed of 92%
6 ACN/20 mM ammonium formate (pH 3.0), the retention factor of nucleosides was
7 higher than that of benzoic acid derivatives, due to the less hydrophilicity/polarity of
8 benzoic acid derivatives. Although 3-HBA has a higher log P than 4-HBA (Table 2),
9 the retention factor of 3-HBA was higher than 4-HBA (Fig. 3B), as opposed to
10 hydrophilic mechanism. However, the retention factor was decreased with the
11 increase of pK_{a2} for the benzoic acid derivatives, with log k' values plotted against the
12 pK_{a2} values for the benzoic acid derivatives (Supplementary Material, Fig. S1). The
13 results indicate a role of the hydrogen bond of analytes in the retention mechanism, as
14 suggested in a previous report [27]. Since VBSIm also contains a butyl group, a
15 hydrophobic interaction mechanism might be exhibited with lower ACN
16 concentrations (e.g. 60%, 30% and 10%). Nucleosides and benzoic acid derivatives
17 were eluted in the dead time with the mobile phase containing either 60% or 30%
18 ACN. However, benzoic acid derivatives were not eluted in a 50 min run with 10%
19 ACN, although nucleosides were also eluted in the dead time. This phenomenon could
20 be simply explained by hydrophobic interaction mechanism of benzoic acid
21 derivatives. However, since the aim of this work was focused on HILIC separation of
22 polar compounds, we did not intend to investigate the potential hydrophobic
23 interaction mechanism of the poly (VBSIm-AM-MBA) monolith in detail. As a result,
24 to obtain better separation efficiency and peak shape, the ACN content of 92% and
25 94% was adopted towards nucleosides and benzoic acid derivatives, respectively.

26
27
28
29
30
31
32
33
34
35
36
37
38
39
40
41
42
43
44
45
46
47 The buffer pH in the mobile phase plays an important role in the separation of
48 nucleosides and benzoic acid derivatives, since it not only determines the state of the
49 analytes in solution as ionic or neutral molecules but also affects the surface charge of
50 the poly (VBSIm-AM-MBA) monolithic column. As shown in Fig. 1, there are
51 several functional groups on the surface of poly (VBSIm-AM-MBA) monolithic
52 column: imidazole group (pK_a 6.7) [28], amine group (pK_a 10.6) [29], and sulfonic
53 group (pK_a 1.2) [21]. With a pH less than 8.6 (pK_a-2 , amine groups), amine groups
54
55
56
57
58
59
60

1
2
3 were positively charged, and imidazole groups were partially positively charged. The
4 sulfonic groups were negatively charged with a pH higher than 3.2 (pK_a 1.2 for
5 sulfonic groups). Since the AM and VBSIm were of equal molar ratio in the poly
6 (VBSIm-AM-MBA) monolithic column, the positive charges on the surface of the
7 monolithic column were decreased with the increase of pH value from 3.0 to 6.5.
8
9

10
11
12 The effect of the mobile phase pH on the retention factor of nucleosides was
13 investigated in a pH range from 3.0 to 6.5 at 20 mM ammonium formate and
14 ACN/water of 92/8 (v/v). As shown in the Fig. 4A, the retention factor of nucleosides
15 was decreased substantially with the increase of mobile phase pH. Given that the pK_{a2}
16 of adenosine, cytosine and cytidine was 3.82, 4.18 and 4.26, respectively (Table 2),
17 the positive charges were decreased with the increase of the buffer pH. The analytes
18 became neutral when the buffer pH was higher than $pK_{a2}+2$. The charged molecules
19 were more hydrophilic than neutral molecules [27]. With the increase of the buffer pH,
20 the hydrophilicity of adenosine, cytosine, cytidine and monolithic column was
21 decreased, resulting in a decreased retention factor. In addition, the positive charge of
22 analytes could interact with the net positive charge of the monolithic column via
23 repulsive electrostatic interaction. With the increase of pH value, analytes and
24 monolithic column were less positively charged, weakening the repulsive electrostatic
25 interaction. However, the hydrophilicity of analytes and monolithic column might be
26 more remarkable than repulsive electrostatic interaction, contributing to weaker
27 retention of the analytes. On the other hand, since the pK_{a1} of uridine and inosine was
28 9.39 and 8.8, respectively, uridine and inosine were neutral with a pH ranged from 3.0
29 to 6.5 ($pH < pK_{a1}-2$). But due to the decreased hydrophilicity of monolithic column
30 with the increase of pH, the retention factors of uridine and inosine were decreased as
31 well.
32
33
34
35
36
37
38
39
40
41
42
43
44
45
46
47
48
49

50 Fig. 4B shows the retention factor changes of benzoic acid derivatives with the
51 mobile phase pH. The retention factors were increased obviously with the increase of
52 pH. Given that the pK_{a1} value for 4-HBA, 3-HBA and 3, 4-HBA was 4.58, 4.08 and
53 4.49, respectively, benzoic acid derivatives could be partially deprotonated in the pH
54 range applied. But with a higher pH, they became more negatively charged, leading to
55
56
57
58
59
60

1
2
3 increased electrostatic interaction between some negative analytes and the net positive
4 charges of monolithic column. As a result, increased retention factors were observed
5 with the increased pH from 3.0 to 5.0.
6
7

8
9 The effect of salt concentration on the retention of nucleosides and benzoic acid
10 derivatives was also investigated, since it not only controls the symmetry of peaks but
11 also affects separation efficiency in HILIC. For the nucleosides analysis, the
12 concentration of ammonium formate (pH 4.0) was varied from 10 to 50 mM, with a
13 constant 92% ACN. For the benzoic acid derivatives analysis, the concentration of
14 ammonium formate (pH 3.0) was varied from 5 to 30 mM, with a constant 94% ACN.
15 As shown in Fig. 5A, with an increase of salt concentration, the retention factors of
16 nucleosides were increased, which might be resulted from the hydrophilic partitioning
17 mechanism [30]. On the other hand, the retention factors of benzoic acid derivatives
18 were increased as the increase of salt concentration from 5 to 20 mM, with the highest
19 retention factors achieved at 20 mM ammonium formate (Fig. 5B), which could also
20 be ascribed to the hydrophilic partitioning mechanism. While the decreasing trend of
21 retention factors can be characteristic of an ion-exchange retention mechanism [31].
22
23
24
25
26
27
28
29
30
31
32
33
34
35

36 **3.3 Reproducibility**

37 Fig. 6 shows the HILIC chromatograms of nucleosides and benzoic acid derivatives
38 under the optimized separation conditions. Baseline separation for five nucleosides
39 and three benzoic acid derivatives was achieved. Since excellent column stability is a
40 prerequisite for its routine application, the run-to-run reproducibility was evaluated on
41 one poly (VBSIm-AM-MBA) monolithic column for 3 runs, with the RSDs for
42 nucleosides ranged from 0.18% to 0.46% (Table 3). Three poly (VBSIm-AM-MBA)
43 monolithic columns prepared in a signal batch were used to evaluate the
44 column-to-column reproducibility, and the RSDs of retention time for the nucleosides
45 were ranged from 2.33% to 4.20% (Table 3). Batch-to batch reproducibility was also
46 evaluated by columns from three different batches, and the RSDs of retention time for
47 the nucleosides were <6.50%.
48
49
50
51
52
53
54
55
56
57
58
59
60

4. Conclusions

A novel zwitterionic poly (VBSIm-AM-MBA) monolithic column, developed by a one-pot copolymerization approach, was used as a stationary phase for capillary HILIC separation of nucleosides and benzoic acid derivatives. The resulting monolithic column exhibited excellent selectivity, efficient retention, and distinguished quantitative analysis for nucleosides and benzoic acid derivatives under the HILIC mode. Nucleosides were retained on the zwitterionic poly (VBSIm-AM-MBA) monolithic column based on the hydrophilic interaction and repulsive electrostatic interaction mechanisms, while benzoic acid derivatives were well separated based on hydrophilic interaction, electronic interaction and hydrogen bonding mechanisms.

Abbreviation

HILIC	Hydrophilic interaction chromatography
RPLC	Reverse phase liquid chromatography
AM	Acrylamide
MBA	<i>N, N'</i> -methylenebisacrylamide
VBSIm	1-Vinyl-3-(butyl-4-sulfonate) imidazolium
ACN	Acetonitrile
PEG	Polyethylene glycol
DMSO	Dimethyl sulphoxide
4-HBA	4-Hydroxybenzoic acid
3-HBA	3-Hydroxybenzoic acid
3, 4-DHBA	3,4- Dihydroxybenzoic acid

Acknowledgements

The project is supported by the National Natural Science Foundation of China (21405085), the Public Applied Research Programs of Technology of Zhejiang Province, the Zhejiang Provincial Natural Science Foundation of China

1
2
3 (LQ12B05001) and the Ningbo Science and Technology Innovation Team
4
5 (2011B82002).
6
7
8

9 10 **References**

- 11 1 B. Buszewski and S. Noga, *Anal. Bioanal. Chem.*, 2012, 402, 231-247.
12
13 2 P. Jandera, *Anal. Chim. Acta*, 2011, 692, 1-25.
14
15 3 A. Shen, Z. Guo, L. Yu, L. Cao and X. Liang, *Chem. Commun.*, 2011, 47,
16 4550-4552.
17
18 4 Y. Li, Y. Feng, T. Chen and H. Zhang, *J. Chromatogr. A*, 2011, 1218, 5987-5994.
19
20 5 X. H. Xiao, L. Zhao, X. Liu and S. X. Jiang, *Anal. Chim. Acta*, 2004, 519, 207-211.
21
22 6 M. J. Ruiz-Angel, S. Carda-Broch and A. Berthod, *J. Chromatogr. A*, 2006, 1119,
23 202-208.
24
25 7 M. T. Ubeda-Torres, C. Ortiz-Bolsico, M. C. García-Alvarez-Coque and M. J.
26 Ruiz-Angel, *J. Chromatogr. A*, 2015, 380, 96-103.
27
28 8 V. Pino and A. M. Afonso, *Anal. Chim. Acta*, 2012, 714, 20-37.
29
30 9 D. S. Van Meter, N. J. Oliver, A. B. Carle, S. Dehm, T. H. Ridgway and A. M.
31 Stalcup, *Anal. Bioanal. Chem.*, 2009, 393, 283-294.
32
33 10 H. Qiu, Q. Jiang, Z. Wei, X. Wang, X. Liu and S. Jiang, *J. Chromatogr. A*, 2007,
34 1163, 63-69.
35
36 11 H. Qiu, A. K. Mallik, T. Sawada, M. Takafuji and H. Ihara, *Chem. Commun.*, 2012,
37 48, 1299-1301.
38
39 12 L. Qiao, A. Dou, X. Shi, H. Li, Y. Shan, X. Lu and G. Xu, *J. Chromatogr. A*, 2013,
40 1286, 137-145.
41
42 13 J. Lin, J. Lin, X. Lin and Z. Xie, *J. Chromatogr. A*, 2009, 1216, 801-806.
43
44 14 Z. Jiang, N. W. Smith, P. D. Ferguson and M. R. Taylor, *Anal. Chem.*, 2007, 79,
45 1243-1250.
46
47 15 V. Škeříková and P. Jandera, *J. Chromatogr. A*, 2010, 1217, 7981-7989.
48
49 16 J. Wang, W. Jia, X. Lin, X. Wu and Z. Xie, *Electrophoresis*, 2013, 34, 3293-3299.
50
51 17 Y. Wang, Q. Deng, G. Fang, M. Pan, Y. Yu and S. Wang, *Anal. Chim. Acta*, 2012,
52
53
54
55
56
57
58
59
60

- 1
2
3 712, 1- 8.
4
5 18 Z. Jiang, N. W. Smith, P. D. Ferguson and M. R. Taylor, *J. Sep. Sci.*, 2009, 32,
6 2544 -2555.
7
8 19 T. T. Wang, J. F. Ma, G. J. Zhu, Y. C. Shan, Z. Liang, L. H. Zhang and Y. K. Zhang,
9 *J. Sep. Sci.*, 2010, 33, 3194-3200.
10
11 20 T. T. Wang, Y. H. Chen, J. F. Ma, M. J. Hu, Y. Li, J. H. Fang and H. Q. Gao, *Anal.*
12 *Bioanal. Chem.*, 2014, 406, 4955-4963.
13
14 21 B. Gu, Z. Chen, C. D. Thulin and M. L. Lee, *Anal. Chem.*, 2006, 78, 3509-3518.
15
16 22 M. Chen, L. Li, B. Yuan, Q. Ma and Y. Feng, *J. Chromatogr. A*, 2012, 1230, 54-60.
17
18 23 A. Podgornik, A. Savnik, J. Jančar and N. L. Krajnc, *J. Chromatogr. A*, 2014, 1333,
19 9-17.
20
21 24 D. Moravcová, M. Haapala, J. Planeta, T. Hyötyläinenc, R. Kostianen and S. K.
22 Wiedmer, *J. Chromatogr. A*, 2014, 1373, 90-96.
23
24 25 L. Qiao, S. Wang, H. Li, Y. Shan, A. Dou, X. Shi and G. Xu, *J. Chromatogr. A.*,
25 2014, 1360, 240-247.
26
27 26 H. Qiu, L. Loukotková, P. Sun, E. Tesařová, Z. Bosáková and D. W. Armstrong, *J.*
28 *Chromatogr. A*, 2011, 1218, 270-279.
29
30 27 G. Greco, S. Grosse and T. Letzel, *J. Chromatogr. A*, 2012, 1235, 60-67.
31
32 28 J. C. Vander Woude, I. Y. Christlieb, G. A. Sicard and R. E. Clark, *J. Thorac.*
33 *Cardiovasc. Surg.*, 1985, 90, 225-234.
34
35 29 P. Das, A. R. Silva, A. P. Carvalho, J. Pires and C. Freire, *Catal. Lett.*, 2009, 129,
36 367-375.
37
38 30 A. J. Alpert, *J. Chromatogr.*, 1990, 499, 177-196.
39
40 31 M. Talebi, R. D. Arrua, A. Gaspar, N. A. Lacher, Q. Wang, P. R. Haddad and E. F.
41 Hilder, *Anal. Bioanal. Chem.*, 2013, 405, 2233-2244.
42
43 32 G. P. Cunngham, G. A. Vidulich and R. L. Kay, *J. Chem. Eng. Data*, 1967, 12,
44 336-337.
45
46 33 H. Vlčková, K. Ježková, K. Stětková, H. Tomšíková, P. Solich and L. Nováková, *J.*
47 *Sep. Sci.*, 2014, 37, 1297-1307.
48
49 34 J. Saurina, S. Hernández-Cassou, R. Tauler and A. Izquierdo-Ridorsa, *Anal. Chim.*
50
51
52
53
54
55
56
57
58
59
60

1
2
3 *Acta*, 2000, 408, 135-143.
4
5
6

7 Fig. 1. Preparatory procedure for the zwitterionic poly (VBSIm-AM-MBA)
8 monolithic column.
9

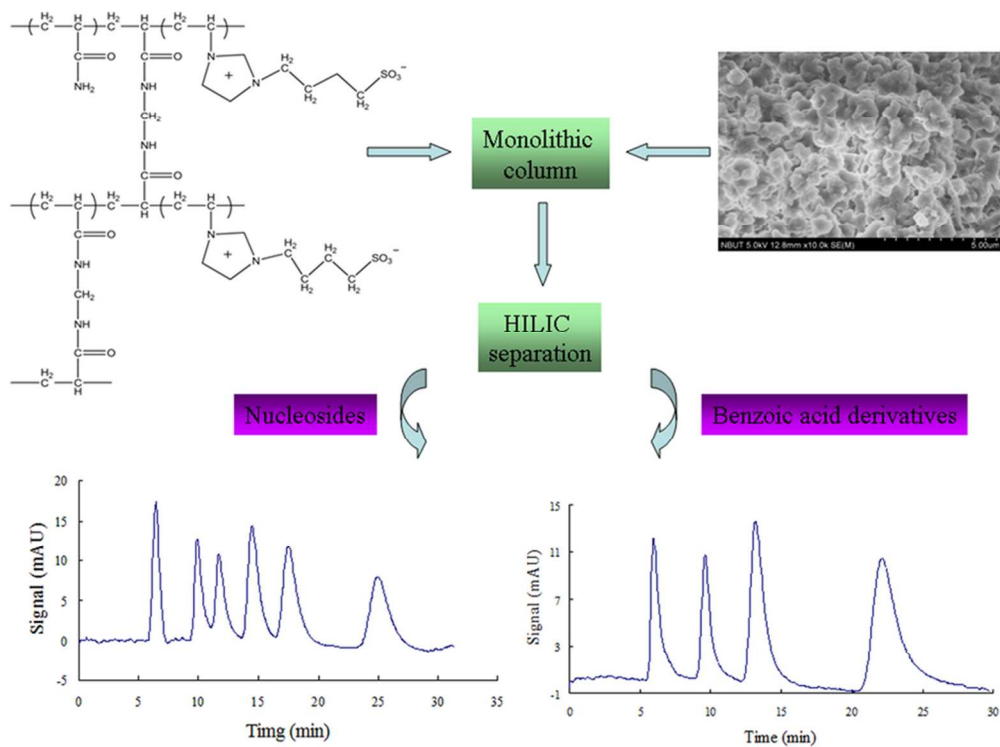
10
11
12 Fig. 2. Scanning electron micrographs of the zwitterionic poly (VBSIm-AM-MBA)
13 monolithic column magnified by 500 (a), 10,000 (b) and 20,000 (c) times.
14
15
16

17
18 Fig. 3. Effect of ACN content on retention factors for nucleosides (a) and benzoic acid
19 derivatives (b).
20
21
22

23
24 Fig. 4. Effect of buffer pH on retention factors for nucleosides (a) and benzoic acid
25 derivatives (b).
26
27
28

29
30 Fig. 5. Effect of buffer salt concentration on retention factors for nucleosides (a) and
31 benzoic acid derivatives (b).
32
33
34

35 Fig.6. HPLC chromatograms of nucleosides (a) and benzoic acid derivatives (b).
36 Order of peaks for (a): (0) Toluene; (1) adenosine; (2) uridine; (3) cytosine; (4)
37 inosine; (5) cytidine. Order of peaks for (b): (0) Toluene; (1) 4-HBA; (2) 3-HBA; (3)
38 3,4-DHBA.
39
40
41
42
43
44
45
46
47
48
49
50
51
52
53
54
55
56
57
58
59
60



Colour graphic
40x30mm (600 x 600 DPI)

1
2
3
4
5
6
7
8
9
10
11
12
13
14
15
16
17
18
19
20
21
22
23
24
25
26
27
28
29
30
31
32
33
34
35
36
37
38
39
40
41
42
43
44
45
46
47
48
49
50
51
52
53
54
55
56
57
58
59
60

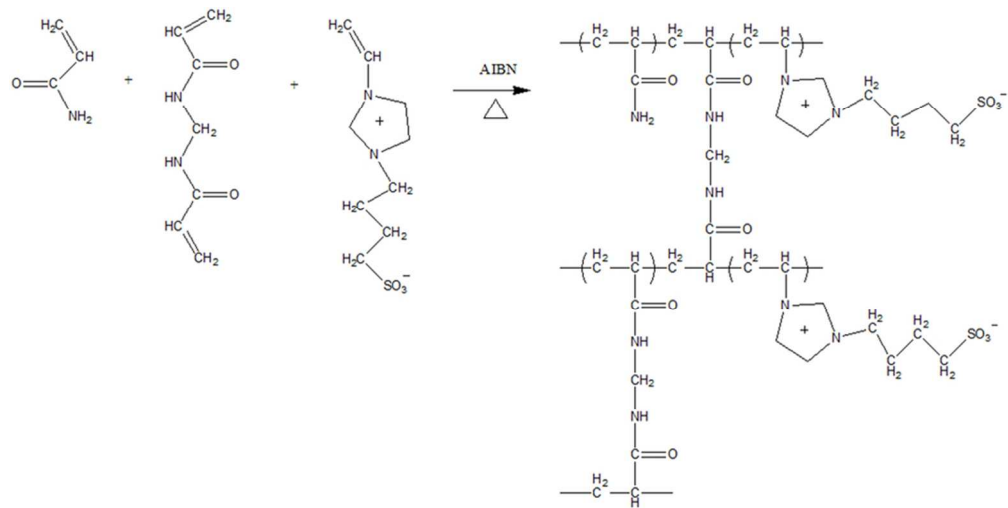


Fig.1
40x20mm (600 x 600 DPI)

1
2
3
4
5
6
7
8
9
10
11
12
13
14
15
16
17
18
19
20
21
22
23
24
25
26
27
28
29
30
31
32
33
34
35
36
37
38
39
40
41
42
43
44
45
46
47
48
49
50
51
52
53
54
55
56
57
58
59
60

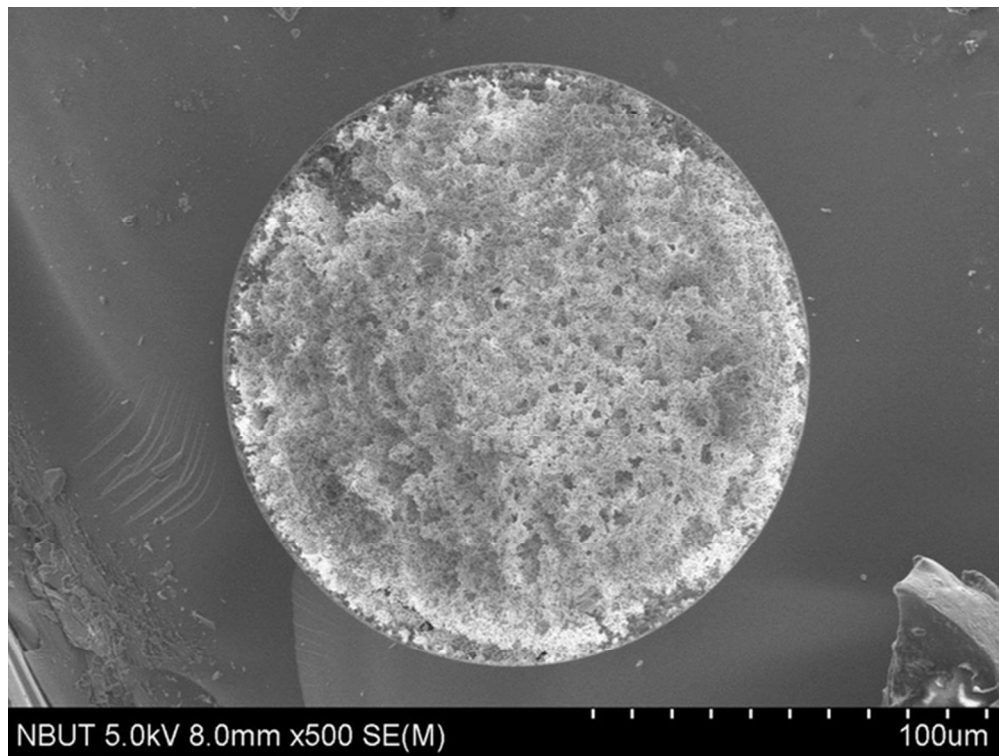


Fig.2a
29x22mm (600 x 600 DPI)

1
2
3
4
5
6
7
8
9
10
11
12
13
14
15
16
17
18
19
20
21
22
23
24
25
26
27
28
29
30
31
32
33
34
35
36
37
38
39
40
41
42
43
44
45
46
47
48
49
50
51
52
53
54
55
56
57
58
59
60

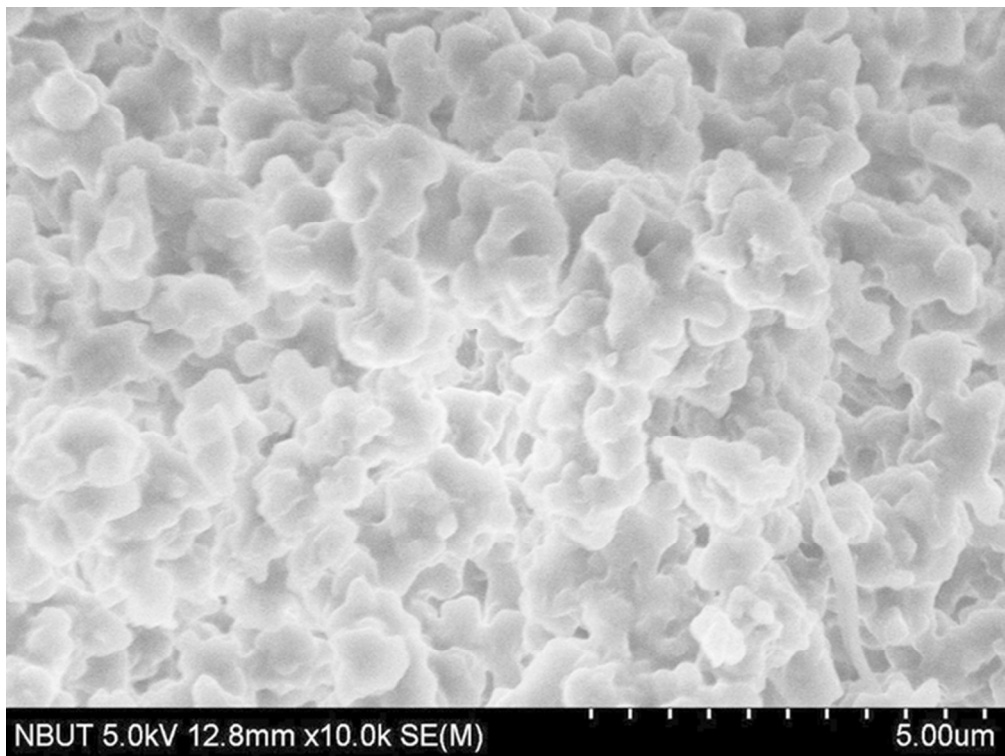


Fig.2b
29x22mm (600 x 600 DPI)

1
2
3
4
5
6
7
8
9
10
11
12
13
14
15
16
17
18
19
20
21
22
23
24
25
26
27
28
29
30
31
32
33
34
35
36
37
38
39
40
41
42
43
44
45
46
47
48
49
50
51
52
53
54
55
56
57
58
59
60

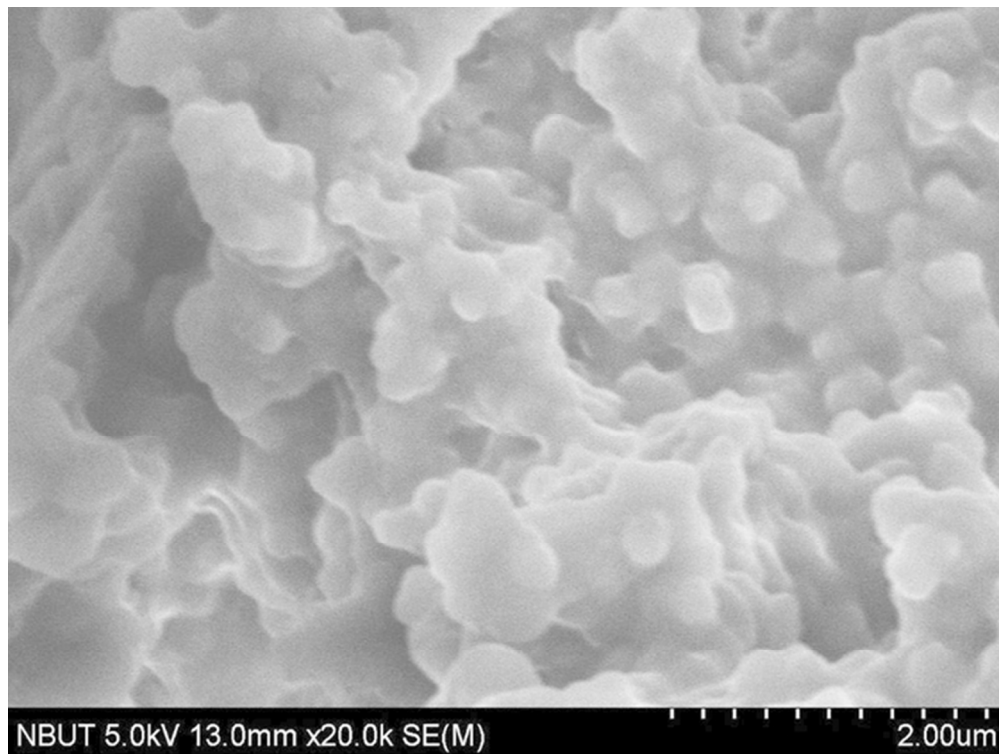


Fig.2c
29x22mm (600 x 600 DPI)

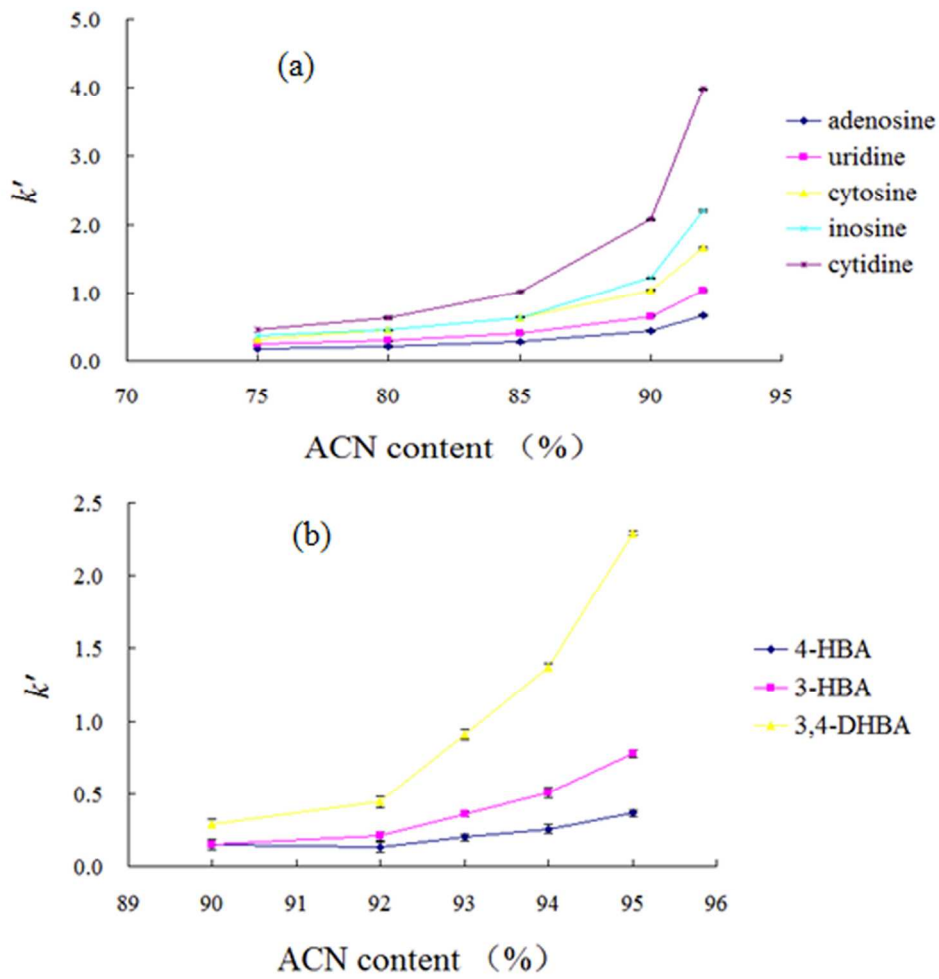


Fig.3
49x48mm (600 x 600 DPI)

1
2
3
4
5
6
7
8
9
10
11
12
13
14
15
16
17
18
19
20
21
22
23
24
25
26
27
28
29
30
31
32
33
34
35
36
37
38
39
40
41
42
43
44
45
46
47
48
49
50
51
52
53
54
55
56
57
58
59
60

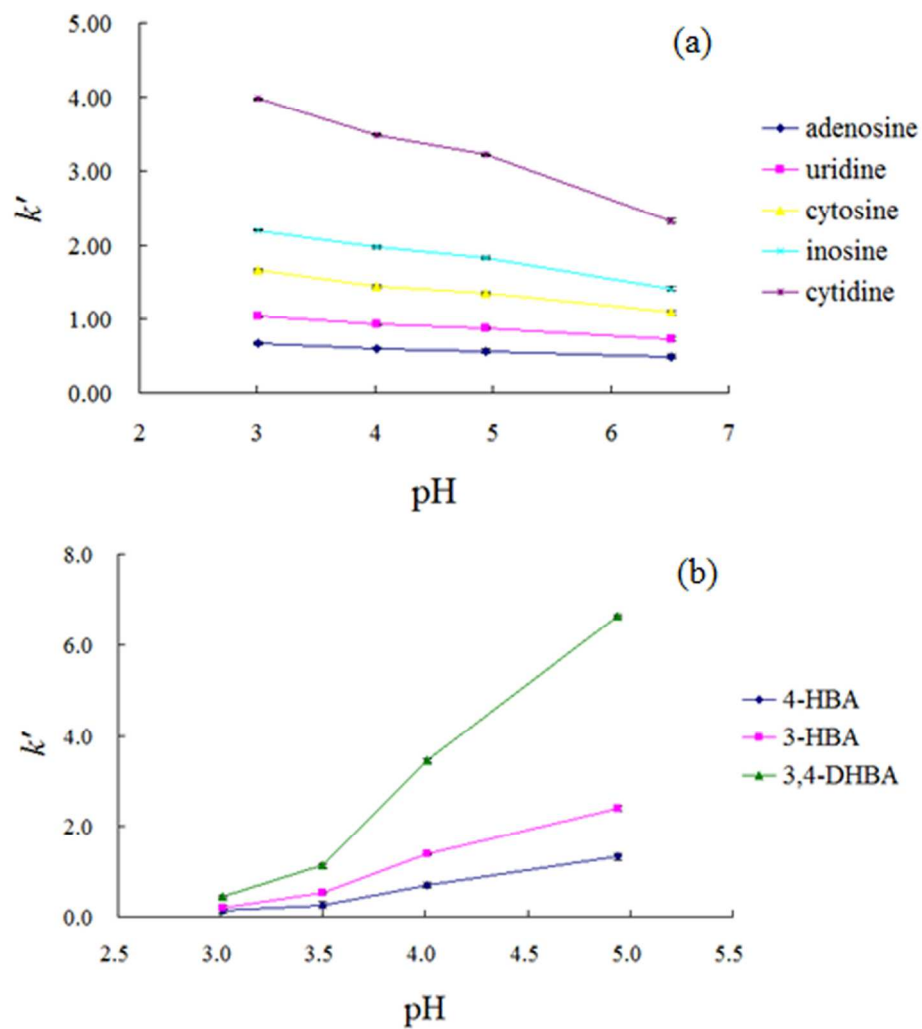


Fig.4
51x53mm (600 x 600 DPI)

1
2
3
4
5
6
7
8
9
10
11
12
13
14
15
16
17
18
19
20
21
22
23
24
25
26
27
28
29
30
31
32
33
34
35
36
37
38
39
40
41
42
43
44
45
46
47
48
49
50
51
52
53
54
55
56
57
58
59
60

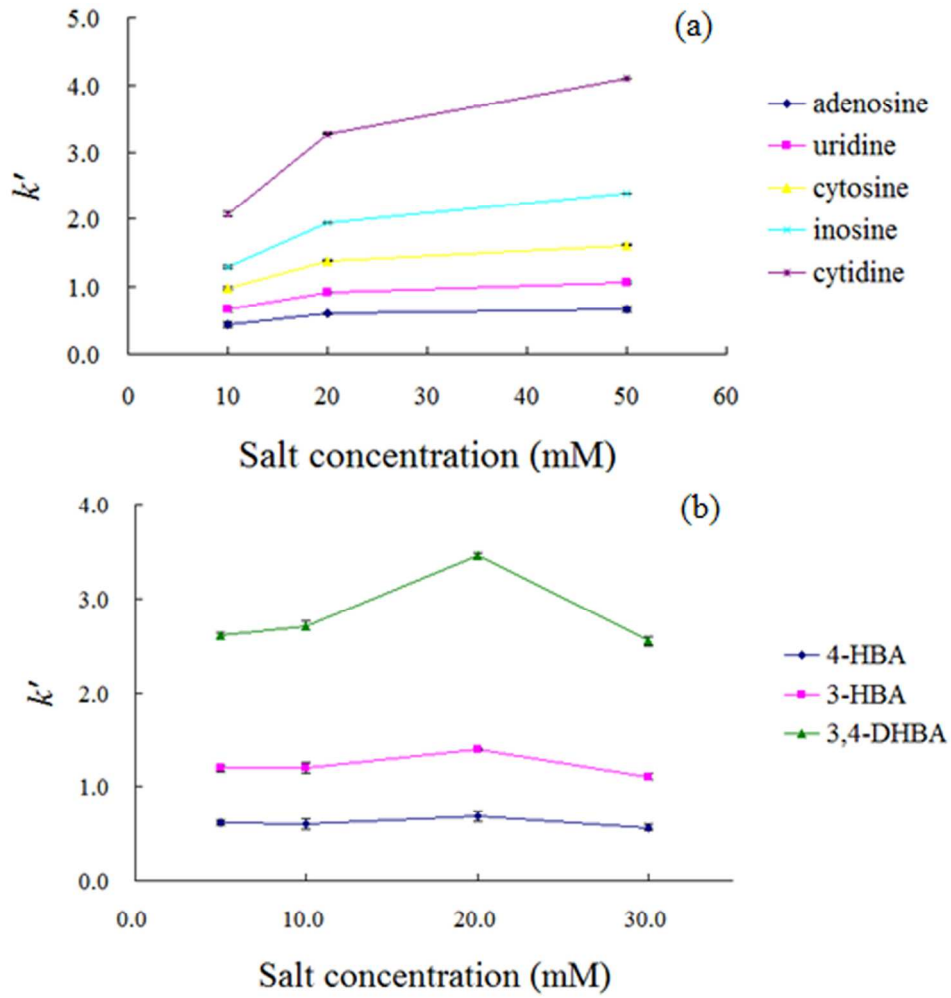


Fig.5
60x60mm (600 x 600 DPI)

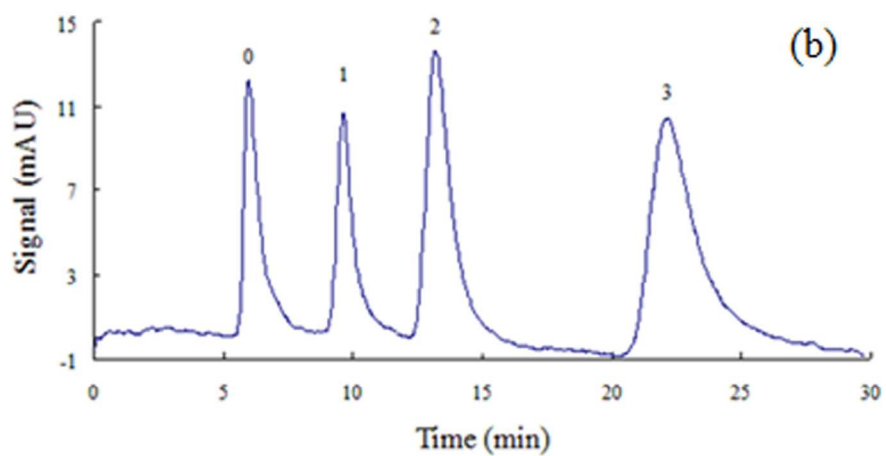
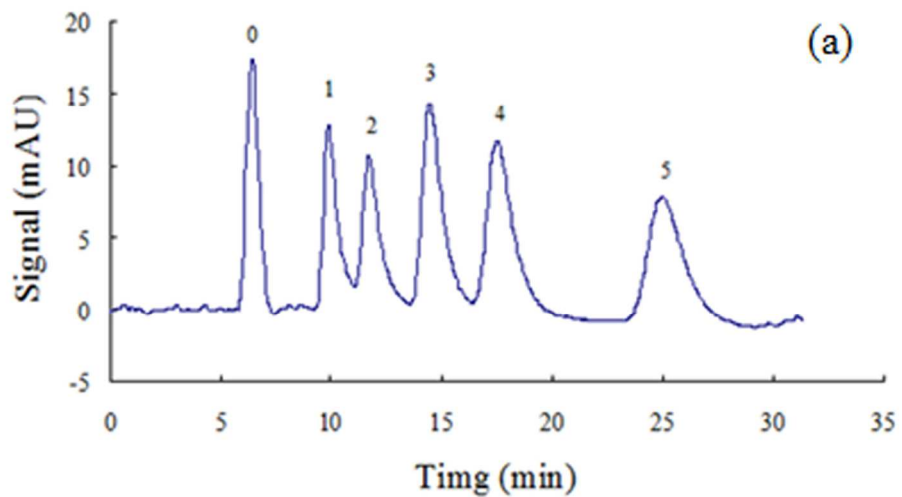


Fig.6
51x54mm (600 x 600 DPI)

1
2
3
4
5
6
7
8
9
10
11
12
13
14
15
16
17
18
19
20
21
22
23
24
25
26
27
28
29
30
31
32
33
34
35
36
37
38
39
40
41
42
43
44
45
46
47
48
49
50
51
52
53
54
55
56
57
58
59
60

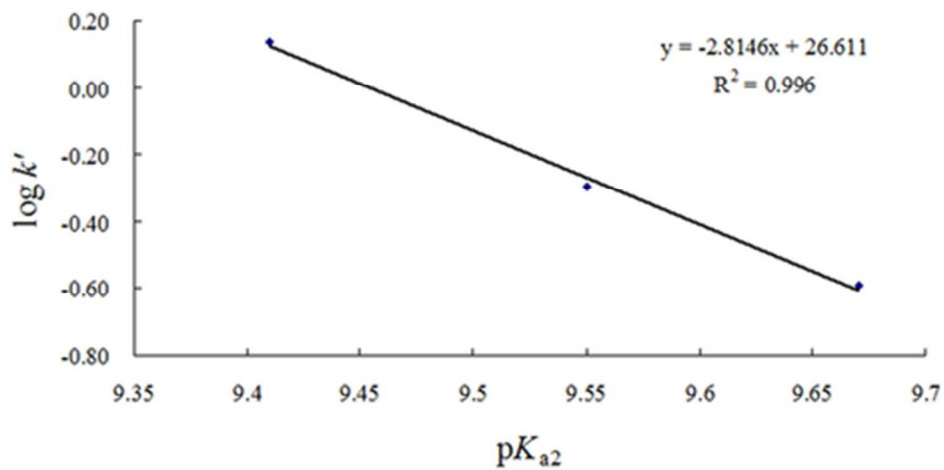


Fig.S1
20x11mm (600 x 600 DPI)

1
2
3
4
5
6
7
8
9
10
11
12
13
14
15
16
17
18
19
20
21
22
23
24
25
26
27
28
29
30
31
32
33
34
35
36
37
38
39
40
41
42
43
44
45
46
47
48
49
50
51
52
53
54
55
56
57
58
59
60

Table 1 Permeability (K) and column efficiency (N) of the monolithic columns with different composition of the polymerization solution

Column	Monomer			Porogenic solvent				K ($\times 10^{-14}$ m^2)	N_{Melamine} (plates/m)	k'_{Melamine}
	AM	MBA	VBSIm	Formamide	DMSO	PEG 8,000	PEG 10,000			
1	10	20	33.4	340	340	45	25	n/a ^a	n/a	n/a
2	10	20	33.4	453.3	226.7	45	25	33.3	2310	0.93
3	10	20	33.4	566.7	113.3	45	25	n/a ^b	n/a	n/a
4	10	20	33.4	453.3	226.7	70	0	12.0	2947	0.97
5	10	20	33.4	453.3	226.7	55	15	33.6	5659	0.87
6	10	20	33.4	453.3	226.7	25	45	34.0	24390	0.87
7	10	20	33.4	453.3	226.7	0	70	55.1	19573	0.94
8	14.5	20	28.9	453.3	226.7	25	45	113	17526	0.72
9	8.7	20	34.7	453.3	226.7	25	45	9.78	2434	1.11
10	7.2	20	36.2	453.3	226.7	25	45	2.28	6331	0.85
11	0	20	43.4	453.3	226.7	25	45	n/a ^a	n/a	n/a
12	10	20	33.4	408	204	22.5	40.5	29.9	33480	1.08
13	10	20	33.4	386.8	193.4	21.3	38.4	22.3	22218	1.09
14	43.4	20	0	408	204	22.5	40.5	17.2	11869	0.60

Capillary column, 30 cm total length \times 150 μm i.d.; Experimental conditions mobile phase: 8% 10 mM ammonium formate (pH 9.0) - 92% ACN (v/v); Flow rate: 1.2 $\mu\text{L}/\text{min}$; **Sample for the column efficiency (N) determination: 2.5 $\mu\text{g mL}^{-1}$ malamine**; The injection volume: 0.2 μL ; The permeability (K) was measured by using 74/26 (v/v) ACN/water. The viscosity of ACN/water (74/26, v/v) was obtained from Ref. [32]. n/a: the measurements could not be made because the columns were not applicable.

^a backpressure too high.

^b Slack, slight detached.

Table 2. Chemical physical data of elected nucleosides and benzoic acid derivatives.

Name	$\text{p}K_{\text{a1}}(\text{acid})$	$\text{p}K_{\text{a2}}(\text{basic})$	$\text{Log } P^{\text{c}}$
Adenosine	13.11 ^a	3.82 ^a	-1.02
Uridine	9.39 ^a	-	-1.61
Cytosine	9.00 ^a	4.18 ^a	-1.71
Inosine	8.8 ^b	-	-1.91
Cytidine	13.48 ^a	4.26 ^a	-1.94
4-HBA	4.58 ^d	9.67 ^d	1.42
3-HBA	4.08 ^d	9.55 ^d	1.50
3,4-HBA	4.49 ^d	9.41 ^d	1.16

^a From Ref. [33].

^b From Ref. [34].

^c Calculated using Advanced Chemistry Development (ACD/Labs) Software V6.0.

^d From Ref. [27].

Table 3 Run-to-run, column-to-column and batch to batch reproducibility expressed as relative standard deviation (RSD) of retention time (n=3).

Analytes	Run-to-run (%)	Column-to-column (%)	Batch to batch (%)
Adenosine	0.18	2.33	3.07
Uridine	0.20	2.83	3.28
Cytosine	0.21	3.34	3.51
Inosine	0.29	3.39	6.50
Cytidine	0.48	4.20	5.94

1
2
3
4
5
6
7
8
9
10
11
12
13
14
15
16
17
18
19
20
21
22
23
24
25
26
27
28
29
30
31
32
33
34
35
36
37
38
39
40
41
42
43
44
45
46
47
48
49
50
51
52
53
54
55
56
57
58
59
60